J|A|C|S
ARTICLES
Published on Web 09/12/2006

# Soluble Narrow Band Gap and Blue Propylenedioxythiophene-Cyanovinylene Polymers as Multifunctional Materials for Photovoltaic and Electrochromic Applications

Barry C. Thompson,[†] Young-Gi Kim,[†] Tracy D. McCarley,[‡] and John R. Reynolds*,[†]

*Contribution from The George and Josephine Butler Polymer Research Laboratory and the Center for Macromolecular Science and Engineering, Department of Chemistry, University of Florida, Gainesville, Florida 32611-7200, and Department of Chemistry, Louisiana State University, Baton Rouge, Louisiana 70803-1804*

Received February 22, 2006; E-mail: reynolds@chem.ufl.edu

***Abstract:*** A family of soluble narrow band gap donor−acceptor conjugated polymers based on dioxythiophenes and cyanovinylenes is reported. The polymers were synthesized using Knoevenagel polycondensation or Yamamoto coupling polymerizations to yield polymers with molecular weights on the order of 10 000−20 000 g/mol, which possess solubility in common organic solvents. Thin film optical measurements revealed narrow band gaps of 1.5−1.8 eV, which gives the polymers a strong overlap of the solar spectrum. The energetic positions of the band edges were determined by cyclic voltammetry and differential pulse voltammetry and demonstrate that the polymers are both air stable and show a strong propensity for photoinduced charge transfer to fullerene acceptors. Such measurements also suggest that the polymers can be both p- and n-type doped, which is supported by spectroelectrochemical results. These polymers have been investigated as electron donors in photovoltaic devices in combination with PCBM ([6,6]-phenyl $C_{61}$-butyric acid methyl ester) as an electron acceptor based on the near ideal band structures designed into the polymers. Efficiencies as high as 0.2% (AM1.5) with short circuit current densities as high as 1.2−1.3 mA/cm$^2$ have been observed in polymer/PCBM (1:4 by weight) devices and external quantum efficiencies of more than 10% have been observed at wavelengths longer than 600 nm. The electrochromic properties of the narrow band gap polymers are also of interest as the polymers show three accessible color states changing from an absorptive blue or purple in the neutral state to a transmissive sky-blue or gray in the oxidized and reduced forms. The wide electrochemical range of electrochromic activity coupled with the strong observed changes in transmissivity between oxidation states makes these materials potentially interesting for application to electrochromic displays.

## Introduction

Conjugated polymers are currently the subject of an intense research effort, primarily focused on the development of electronic and electrochemical devices such as light emitting diodes (LEDs),[1] photovoltaic devices (PVDs),[2] field effect transistors (FETs),[3] and electrochromic devices (ECDs).[4] For any application, it is the ability to tailor the electronic and material properties of conjugated polymers via the organic structure that makes this class of polymer the focus of such a broad research effort. For device applications, it is especially important to control the electronic band structure of the polymer to achieve a band gap of the desired magnitude and frontier orbitals, HOMO (highest occupied molecular orbital) and LUMO (lowest unoccupied molecular orbital) (or band edges), of the proper energies. Developing methodologies to attain such

[†] University of Florida.
[‡] Louisiana State University.

(1) (a) Evans, N. R.; Devi, L. S.; Mak, C. S. K.; Watkins, S. E.; Pascu, S. I.; Kohler, A.; Friend, R. H.; Williams, C. K.; Holmes, A. B. *J. Am. Chem. Soc.* **2006**, *128*, 6647−6656. (b) Niu, Y.-H.; Jen, A. K.-Y. Shu, C. *J. Phys. Chem. B* **2006**, *110*, 6010−6014. (c) Huang, Q.; Evmenenko, G. A.; Dutta, P.; Lee, P.; Armstrong, N. R.; Marks, T. J. *J. Am. Chem. Soc.* **2005**, *127*, 10227−10242. (d) Breen, C. A.; Tischler, J. R.; Bulovic, V.; Swager, T. M. *Adv. Mater.* **2005**, *17*, 1981−1985. (e) Perepichka, I. F.; Perepichka, D. F.; Meng, H.; Wudl, F. *Adv. Mater.* **2005**, *17*, 2281−2305. (f) Jacob, J.; Sax, S.; Piok, T.; List, E. J. W.; Grimsdale, A. C.; Mullen, K. *J. Am. Chem. Soc.* **2004**, *126*, 6987−6995. (g) Ego, C.; Marsitzky, D.; Becker, S.; Zhang, J.; Grimsdale, A. C.; Mullen, K.; MacKenzie, J. D.; Silva, C.; Friend, R. H. *J. Am. Chem. Soc.* **2003**, *125*, 437−443. (h) Akcelrud, L. *Prog. Polym. Sci.* **2003**, *28*, 875−962. (i) Friend, R. H.; Gymer, R. W.; Holmes, A. B.; Burroughes, J. H.; Marks, R. N.; Taliani, C.; Bradley, D. D. C.; Dos Santos, D. A.; Bredas, J. L.; Logdlund, M.; Salaneck, W. R. *Nature* **1999**, *397*, 121−128. (j) Kraft, A.; Grimsdale, A. C.; Holmes, A. B. *Angew. Chem., Int. Ed.* **1998**, *37*, 403−428.

(2) (a) Scharber, M. C.; Muhlbacher, D.; Koppe, M.; Denk, P.; Waldauf, C.; Heeger, A. J.; Brabec, C. J. *Adv. Mater.* **2006**, *18*, 789−794. (b) Kim, J. Y.; Kim, S. H.; Lee, H.-H.; Lee, K.; Ma, W.; Gong, X.; Heeger, A. J. *Adv. Mater.* **2006**, *18*, 572−576. (c) Kim, Y.; Cook, S.; Tuladhar, S. M.; Choulis, S. A.; Nelson, J.; Durrant, J. R.; Bradley, D. D. C.; Giles, M.; McCulloch, I.; Ha, C.-S.; Ree, M. *Nat. Mater.* **2006**, *5*, 197−203. (d) Hou, J.; Tan, Z.; Yan, Y.; He, Y.; Yang, C.; Li, Y. *J. Am. Chem. Soc.* **2006**, *128*, 4911−4916. (e) Koetse, M. M.; Sweelssen, J.; Hoekerd, K. T.; Schoo, H. F. M.; Veenstra, S. C.; Kroon, J. M.; Yang, X.; Loos, J. *Appl. Phys. Lett.* **2006**, *88*, 083504. (f) Shrotriya, V.; Wu, E. H.-E.; Li, G.; Yao, Y.; Yang, Y. *Appl. Phys. Lett.* **2006**, *88*, 064104. (g) Beek, W. J. E.; Sloof, L. H.; Wienk, M. M.; Kroon, J. M.; Janssen, R. A. J. *Adv. Funct. Mater.* **2005**, *15*, 1703−1707. (h) Coakley, K. M.; McGehee, M. D. *Chem. Mater.* **2004**, *16*, 4533−4542. (i) Hoppe, H.; Sariciftci, N. S. *J. Mater. Res.* **2004**, *19*, 1924−1945. (j) Brabec, C. J.; Sariciftci, N. S.; Hummelen, J. C. *Adv. Funct. Mater.* **2001**, *11*, 15−26.


**10.1021/ja061274a CCC: $33.50** 

precise control over the polymer electronic structure is a key aspect for the advancement of the field.[5] Equally important is the control of a materials physical properties. The development of novel polymers that are soluble in common organic solvents and processable by industrially relevant techniques, such as spin-coating, spray-coating, screen-printing, inkjet-printing, or roller coating, is necessary for the practical application of conjugated polymers. Such processable polymers with tailored electronic structures also possess the possibility to be multifunctional materials that can find application in numerous device architectures.

An especially interesting class of conjugated polymer are the soluble, narrow band gap polymers. Such polymers offer a broad range of attractive features for use in a variety of device architectures, such as a strong overlap with the solar spectrum (PVDs), ease of oxidation and reduction (ECDs) as well as the potential for high electron and hole mobility (PVDs, TFTs, and LEDs), and a potentially transparent oxidized state (ECDs). Although several approaches have been taken toward the development of narrow band gap polymers,[5b,6] soluble and processable systems are rare. Four main approaches toward the development of soluble, narrow band gap polymers dominate the literature. The first is based specifically on the development of poly(thienylenevinylene) polymers and analogues,[7] for which band gaps of 1.6−1.8 eV are commonly observed. The second approach is based on decreasing the band gap by increasing the quinoidal character of the polymer backbone, and this approach is primarily based on poly(isothionaphthene),[8] along with poly(arylene methine)[9] and poly(thieno[3,4b]thiophene),[10] polymers. A third route is based on the control of regioregularity in polythiophenes. In this case, band gaps as low as 1.4 eV have been realized for the case of regioregular poly(3-alkoxythiophenes).[11] A more general route is the donor−acceptor (DA) approach,[5b,6c] which has proven especially successful for the development of electropolymerizable polymers with band gaps as low as 0.3−0.5 eV.[12] Several types of soluble narrow band gap DA polymers have been reported, especially for use in PVDs.[13] Band gaps as low as 1.3 eV have been reported for alternating copolymers of dialkyl fluorene and bis-thienylthiadiazoloquinoxaline[14] and 1.5 eV for alternating copolymers of bis-thienyl-*N*-alkylpyrroles and benzothiadiazole.[15] Another class of DA polymers are based on cyanovinylene (CNV) as an acceptor used in concert with electron-rich aromatics. Band gaps as low as 1.1 eV have been reported for electropolymerized bis-(3,4-ethylenedioxythiophene)-CNV (BEDOT-CNV) polymers.[16] The primary route to soluble CNV polymers has been through the Knoevenagel polycondensation polymerization.[17] In the case of CN−PPV (Figure 1), a band gap of 2.1 eV is observed when dialkoxybenzene is used as the donor. This band gap is not reduced relative to MEH−PPV based on the relatively weak donor nature of dialkoxybenzene, although replacing one or both dialkoxybenzenes with alkylthiophenes has led to band gaps of 1.8 and 1.6 eV, respectively.[18] Soluble, narrow band gap CNV polymers based on 3,4-ethylenedioxythiophene (EDOT) with band gaps as low as 1.6 eV have also been realized by oxidative polymerization of bis-heterocycle-CNV monomers.[19]

The major advantage of the DA approach is that proper choice of the donor and acceptor groups allows one to select the approximate HOMO and LUMO energies of the resulting polymer. This is especially attractive for the development of


(3) (a) McCulloch, I.; Heeney, M.; Bailey, C.; Genevicius, K.; MacDonald, I.; Shkunov, M.; Sparrowe, D.; Tierney, S.; Wagner, R.; Zhang, W.; Chabinyc, M. L.; Kline, R. J.; McGehee, M. D.; Toney, M. F. *Nat. Mater.* **2006**, *5*, 328−333. (b) Kline, R. J.; McGehee, M. D.; Toney, M. F. *Nat. Mater.* **2006**, *5*, 222−228. (c) Sirringhaus, H. *Adv. Mater.* **2005**, 17, 2411−2425. (d) Chua, L.-L.; Zaumseil, J.; Chang, J.-F.; Ou, E. C.-W.; Ho, P. K.-H.; Sirringhaus, H.; Friend, R. H. *Nature* **2005**, *434*, 194−199. (e) Murphy, A. R.; Liu, J.; Luscombe, C.; Kavulak, D.; Fréchet, J. M. J.; Kline, R. J.; McGehee, M. D. *Chem. Mater.* **2005**, *17*, 4892−4899. (f) Wu, Y.; Liu, P.; Ong, B. S.; Srikumar, T.; Zhao, N.; Botton, G.; Zhu, S. *Appl. Phys. Lett.* **2005**, 86, 142102, (g) Stutzmann, N.; Friend, R. H.; Sirringhaus, H. *Science* **2003**, *299*, 1881−1884. (h) Sirringhaus, H.; Brown, P. J.; Friend, R. H.; Nielsen, M. M.; Bechgaard, K.; Langeveld, B. M. W.; Spiering, A. J. H.; Janssen, R. A. J.; Meijer, E. W.; Herwig, P.; de Leeuw, D. M. *Nature* **1999**, *401*, 685−688.

(4) (a) Mortimer, R. J.; Dyer, A. L.; Reynolds, J. R. *Displays* **2006**, *27*, 2−18. (b) Sonmez, G.; *Chem. Commun.* **2005**, 5251−5259. (c) Ko, H. C.; Kim, S.; Lee, H.; Moon, B. *Adv. Funct. Mater.* **2005**, *15*, 905−909. (d) Argun, A. A.; Aubert, P.-H.; Thompson, B. C.; Schwendeman, I.; Gaupp, C. L.; Hwang, J.; Pinto, N. J.; Tanner, D. B.; MacDiarmid, A. G.; Reynolds, J. R. *Chem. Mater.* **2004**, *16*, 4401−4412. (e) Sonmez, G.; Meng, H.; Wudl, F. *Chem. Mater.* **2004**, *16*, 574−580. (f) Fungo, F.; Jenekhe, S. A.; Bard, A. J. *Chem. Mater.* **2003**, *15*, 1264−1272.

(5) (a) Moliton, A.; Hiorns, R. C. *Polym. Int.* **2004**, *53*, 1397−1412. (b) Roncali, J. *Chem. Rev.* **1997**, *97*, 173−205.

(6) (a) Kertesz, M.; Choi, C. H.; Yang, S. *Chem. Rev.* **2005**, *105*, 3448−3481. (b) Ajayaghosh, A. *Chem. Soc. Rev.* **2003**, *32*, 181−191. (c) van Mullekom, H. A. M.; Vekemans, J. A. J. M.; Havinga, E. E.; Meijer, E. W. *Mater. Sci. Eng.* **2001**, *32*, 1−40.

(7) (a) Berridge, R.; Skabara, P. J.; Pozo-Gonzalo, C.; Kanibolotsky, A.; Lohr, J.; McDouall, J. J. W.; McInnes, E. J. L.; Wolowska, J.; Winder, C.; Sariciftci, N. S.; Harrington, R. W.; Clegg, W. *J. Phys. Chem. B* **2006**, *110*, 3140−3152. (b) Henckens, A.; Colladet, K.; Fourier, S.; Cleij, T. J.; Lutsen, L.; Gelan, J.; Vanderzande, D. M*acromolecules* **2005**, *38*, 19−26. (c) Henckens, A.; Knipper, M.; Polec, I.; Manca, J.; Lutsen, L.; Vanderzande, D. *Thin Solid Films* **2004**, *451*−*452*, 572−579. (d) Smith, A. P.; Smith, R. R.; Taylor, B. E.; Durstock, M. F. *Chem. Mater.* **2004**, *16*, 4687−4692. (e) Kim, I. T.; Elsenbaumer, R. L. *Macromolecules* **2000**, *33*, 6407−6411. (f) Jen, K. W.; Maxfield, M.; Shacklette, L. W.; Elsenbaumer, R. L. *J. Chem. Soc. Chem. Commun.* **1987**, 309−311.

(8) (a) Polec, I.; Henckens, A.; Goris, L.; Nicolas, M.; Loi, M. A.; Adriaensens, P. J.; Lutsen, L.; Manca, J. V.; Vanderzande, D.; Sariciftci, N. S. *J. Polym. Sci. Part A: Polym. Chem.* **2003**, *41*, 1034−1045. (b) Meng, H.; Tucker, D.; Chaffins, S.; Chen, Y.; Helgeson, R.; Dunn, B.; Wudl, F. *Adv. Mater.* **2003**, *15*, 146−149. (c) Meng, H.; Wudl, F. *Macromolecules* **2001**, *34*, 1810−1816.

(9) (a) Zaman, M. B.; Perepichka, D. F. *Chem. Commun.* **2005**, 4187−4189. (b) Chen, W.-C.; Liu, C.-L.; Yen, C.-T.; Tsai, F.-C.; Tonzola, C. J.; Olson, N.; Jenekhe, S. A. *Macromolecules* **2004**, *37*, 5959−5964. (c) Kiebooms, R. H. L.; Goto, H.; Akagi, K. *Macromolecules* **2001**, *34*, 7989−7998. (d) Chen, W.-C.; Jenekhe, S. A. *Macromolecules* **1995**, *28*, 454−464. (e) Chen, W.-C.; Jenekhe, S. A. *Macromolecules* **1995**, *28*, 465−480.

(10) (a) Kumar, A.; Buyukmumeu, Z.; Sotzing, G. A. *Macromolecules* **2006**, *39*, 2723−2725. (b) Lee, K.; Sotzing, G. A. *Macromolecules* **2001**, *34*, 5746−5747. (c) Pomerantz, M.; Gu, X.; Zhang, S. X. *Macromolecules* **2001**, *34*, 1817−1822.

(11) Sheina, E. E.; Khersonsky, S. M.; Jones, E. G.; McCullough, R. D. *Chem. Mater.* **2005**, *17*, 3317−3319.

(12) (a) Tanaka, S.; Yamashita, Y. *Synth. Met.* **1995**, *69*, 599−600. (b) Kitamura, C.; Tanaka, S.; Yamashita, Y. *Chem. Mater.* **1996**, *8*, 570−578.

(13) (a) Wienk, M. M.; Turbiez, M. G. R.; Struijk, M. P. *Appl. Phys. Lett.* **2006**, *88*, 153511. (b) Bundgaard, E.; Krebs, F. C. *Macromolecules* **2006**, *39*, 2823−2831. (c) Zhang, F.; Jespersen, K. G.; Bjorstrom, C.; Svensson, M.; Andersson, M. R.; Sundstrom, V.; Magnusson, K.; Moons, E.; Yartsev, A.; Inganas, O. *Adv. Funct. Mater.* **2006**, *16*, 667−674. (d) Campos, L. M.; Tontcheva, A.; Gunes, S.; Sonmez, G.; Neugebauer, H.; Sariciftci, N. S.; Wudl, F. *Chem. Mater.* **2005**, *17*, 4031−4033. (e) Kenning, D. D.; Rasmussen, S. C. *Macromolecules* **2003**, *36*, 6298−6299.

(14) Chen, M.; Perzon, E.; Andersson, M. R.; Marcinkevicius, S.; Jonsson, S. K. M.; Fahlman, M.; Berggren, M. *Appl. Phys. Lett.* **2004**, *84*, 3570−3572.

(15) Dhanabalan, A.; van Duren, J. K. J.; van Hal, P. A.; van Dongen, J. L. J.; Janssen, R. A. J. *Adv. Funct. Mater.* **2001**, *11*, 255−262.

(16) Thomas, C. A.; Zong, K.; Abboud, K. A.; Steel, P. J.; Reynolds, J. R. *J. Am. Chem. Soc.* **2004**, *126*, 16440−16450.

(17) (a) Taranekar, P.; Abdulbaki, M.; Krishnamoorti, R.; Phanichphant, S.; Waenkaew, P.; Patton, D.; Fulghum, T.; Advincula, R. *Macromolecules* **2006**, *39*, 3848−3854. (b) Morin, J.-F.; Drolet, N.; Tao, Y.; Leclerc, M. *Chem. Mater.* **2004**, *16*, 4619−4626. (c) Boucard, V. *Macromolecules* **2001**, *34*, 4308−4313. (d) Li, X.-C.; Liu, Y.; Liu, M. S.; Jen, A. K.-Y. *Chem. Mater.* **1999**, *11*, 1568−1575. (e) Kim, K.-D.; Park, J.-S.; Kim, H. K.; Lee, T. B.; No, K. T. *Macromolecules* **1998**, *31*, 7267−7272. (f) Greenham, N. C.; Moratti, S. C.; Bradley, D. D. C.; Friend, R. H.; Holmes, A. B. *Nature* **1993**, *365*, 628−630.

(18) Moratti, S. C.; Cervini, R. Holmes, A. B.; Baigent, D. R.; Friend, R. H.; Greenham, N. C.; Gruner, J.; Hamer, P. J. *Synth. Met.* **1995**, *71*, 2117−2120.

(19) Colladet, K.; Nicolas, M.; Goris, L.; Lutsen, L.; Vanderzande, D. *Thin Solid Films* **2004**, *451*−*452*, 7−11.

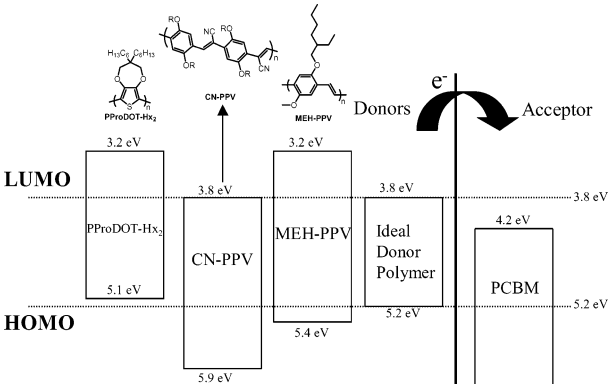


***Figure 1.*** Band diagram for an ideal donor polymer for PCBM. Also shown are donors MEH−PPV, CN−PPV, and PProDOT-$Hx_2$. Dashed lines indicate the thresholds for air stability (5.2 eV) and effective charge transfer to PCBM (3.8 eV). Note that these values are all approximate as some values come from the literature and the method of determining HOMO−LUMO energies varies from sample to sample. In all cases, orbital energies are given based on the assumption that the energy of SCE is 4.7 eV vs vacuum,[20] and Fc/$Fc^+$ is +0.380 V vs SCE[21] (i.e., 5.1 eV relative to vacuum).

polymers for electronic device applications, such as PVDs. At the present time, conjugated polymer-based PVDs are able to give efficiencies of 2.5−5.0%.[22] The best results are achieved with so-called bulk-heterojunction devices based on dialkoxy-PPVs (MEH−PPV or MDMO−PPV) or poly(3-alkylthiophenes) (P3AT) as donors in combination with soluble fullerene acceptors, most notably PCBM.[23] By optimizing film morphology and composition as well as device construction (choice of electrodes, buffer layers, etc.), efficiency appears to peak at ∼5%. One deficiency in the operation of PPV or P3AT devices is the limitation induced by the relatively high polymer band gaps of 2.2 and 2.0 eV, respectively. Although the peak of photon flux from the sun occurs at ∼1.8 eV (700 nm), such polymers do not have an appreciable absorbance in this wavelength range. To increase the number of photons absorbed at peak solar wavelengths, it is necessary to shift the absorbance spectrum of the donor polymer toward the red end of the visible spectrum, and thus, the synthesis of new, narrow band gap polymers is required.[24]

However, possessing a narrow band gap is not sufficient to ensure that a polymer will give optimal or ideal performance in a solar cell, as the positions of the frontier orbitals are also critical to ensure effective charge transfer and collection. To the best of our knowledge, no systematic approach for the development of an "ideal" narrow band gap donor polymer has been published. An ideal donor polymer can be defined as a polymer with the minimal band gap allowed by frontier orbital requirements for air stability and charge transfer to a given acceptor. The polymer must also exhibit suitably high hole mobility to work effectively in concert with the acceptor for charge transport in a device.[25] Our approach to an ideal donor, communicated recently,[26,27] is outlined below. Here, optimization of hole mobility is considered a second level of polymer modification in structures that exhibit an ideal electronic structure. Figure 1 illustrates the band structure of several polymers including MEH−PPV and an ideal donor relative to PCBM. To arrive at the ideal donor band structure, it is first desired that a polymer be air stable (i.e., resistant to oxidation) to allow ease of handling and processing by having a fairly low-lying HOMO (∼5.2 eV or lower,[28] assuming that the energy level of SCE is 4.7 eV[20] below the vacuum level). Additionally, a donor polymer intended for use with a fullerene acceptor should be capable of electron transfer to the fullerene upon photoexcitation. As an approximation, electron transfer is assumed possible if the band offset between the donor LUMO and the acceptor LUMO is greater than the exciton binding energy, estimated to be 0.4−0.5 eV,[29] although LUMO offsets of as little as 0.3 eV have been shown sufficient for photoinduced electron transfer.[30] Thus, the donor polymer should have a LUMO energy of 3.8 eV or above, for the case of a PCBM acceptor (LUMO = 4.2 eV). To transform MEH−PPV into an ideal donor for PCBM, the LUMO must be lowered from 3.2 to ∼3.8 eV. The ideal donor polymer, with a LUMO of 3.8 eV and a HOMO of 5.2 eV, will allow a minimal band gap (∼1.4 eV), without appreciably compromising the $V_{oc}$ of the PVD (the $V_{oc}$ is thought to be related to the energetic difference between the donor HOMO and the acceptor LUMO, although the work functions of the electrodes do play a role[24]).

As one avenue toward the conversion of dialkoxy-PPV into an ideal donor, the replacement of vinylene linkages with cyanovinylene linkages is known to lower both the LUMO and the HOMO by ∼0.5 eV, as seen for CN−PPV in Figure 1. The incorporation of an electron-rich moiety in place of a dialkoxybenzene should cause the HOMO of the polymer to be raised relative to that of CN−PPV while relying on the stronger donor−acceptor interaction to concomitantly compress the band gap and approximate the ideal donor. An advantage of this approach is that little effect on the LUMO energy of CN−PPV is expected upon increasing the electron richness of the backbone, as detailed work by our group has shown that in a homologous series of donor−acceptor CNV polymers, the donor strength controls the HOMO energy without significantly affecting the acceptor determined LUMO energy.[16] As CN−PPV has a LUMO of ∼3.8 eV, this route appears promising.

(20) Hansen, W. N.; Hansen, G. J. *Phys. Rev. A: At., Mol., Opt. Phys.* **1987**, *36*, 1396−1402.
(21) Pavlishchuk, V. V.; Addison, A. W. *Inorg. Chim. Acta* **2000**, *298*, 97−102.
(22) (a) Al-Ibrahim, M.; Ambacher, O.; Sensfuss, S.; Gobsch, G. *Appl. Phys. Lett.* **2005**, *86*, 201120. (b) Schilinsky, P.; Asawapirom, U.; Scherf, U.; Biele, M.; Brabec, C. J. *Chem. Mater.* **2005**, *17*, 2175−2180. (c) Kim, Y.; Choulis, S. A.; Nelson, J.; Bradley, D. D. C.; Cook, S.; Durrant, J. R. *Appl. Phys. Lett.* **2005**, *86*, 063502. (d) Brabec, C. J. *Sol. Energy Mater. Sol. Cells* **2004**, *83*, 273−292. (e) Alem, S.; de Bettignies, R.; Nunzi, J.-M.; Cariou, M. *Appl. Phys. Lett.* **2004**, *84*, 2178−2180. (f) Padinger, F.; Rittberger, R. S.; Sariciftci, N. S. *Adv. Funct. Mater.* **2003**, *13*, 85−88. (g) Wienk, M. M.; Kroon, J. M.; Verhees, W. J. H.; Knol, J.; Hummelen, J. C.; van Hal, P. A.; Janssen, R. A. J. *Angew. Chem., Int. Ed.* **2003**, *42*, 3371−3375. (h) Shaheen, S. E.; Brabec, C. J.; Sariciftci, N. S.; Padinger, F.; Fromherz, T.; Hummelen, J. C. *Appl. Phys. Lett.* **2001**, *78*, 841−843. (i) Reyes-Reyes, M.; Kim, K.; Carroll, D. L. *Appl. Phys. Lett.* **2005**, *87*, 083506. (j) Li, G.; Shrotriya, V.; Huang, J.; Yao, Y.; Moriarty, T.; Emery, K.; Yang, Y. *Nat. Mater.* **2005**, *4*, 864−868. (k) Ma, W.; Yang, C.; Gong, X.; Lee, K.; Heeger, A. J. *Adv. Funct. Mater.* **2005**, *15*, 1617−1622.
(23) Hummelen, J. C.; Knight, B. W.; Lepec, F.; Wudl, F. *J. Org. Chem.* **1995**, *60*, 532−538.
(24) Winder, C.; Sariciftci, N. S. *J. Mater. Chem.* **2004**, *14*, 1077−1086.
(25) Melzer, C.; Koop, E. J.; Mihailetchi, V. D.; Blom, P. W. M. *Adv. Funct. Mater.* **2004**, *14*, 865−870.
(26) Thompson, B. C.; Kim, Y. G.; Reynolds, J. R. *Macromolecules* **2005**, *38*, 5359−5362.
(27) Kim, Y.-G.; Thompson, B. C.; Ananthakrishnan, N.; Padmanaban, G.; Ramakrishnan, S.; Reynolds, J. R. *J. Mater. Res.* **2005**, *20*, 3188−3198.
(28) de Leeuw, D. M.; Simenon, M. M. J.; Brown, A. R.; Einerhard, R. E. F. *Synth. Met.* **1997**, *87*, 53−59.
(29) (a) Arkhipov, V. I.; Bassler, H. *Phys. Stat. Sol.* **2004**, *201*, 1152−1187. (b) Meskers, S. C. J.; Hubner, J.; Oestreich, M.; Bassler, H. *J. Phys. Chem. B* **2001**, *105*, 9139−9149.
(30) (a) Brabec, C. J.; Winder, C.; Sariciftci, N. S.; Hummelen, J. C.; Dhanabalan, A.; van Hal, P. A.; Janssen, R. A. J. *Adv. Funct. Mater.* **2002**, *12*, 709−712. (b) Winder, C.; Matt, G.; Hummelen, J. C.; Janssen, R. A. J.; Sariciftci, N. S.; Brabec, C. J. *Thin Solid Films* **2002**, *403*−*404*, 373−379.

***Scheme 1***

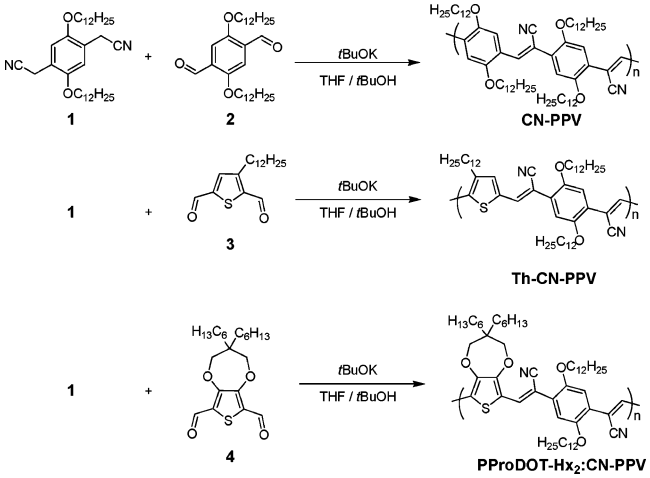


Although CNV is typically a structural motif used in electron accepting polymers, CNV polymers have been used as donors in PCBM-based photovoltaic devices, albeit with limited success.[31] In the design of the ideal donor using CN−PPV as the parent structure, our primary choice for the electron-rich donor moiety used for replacing dialkoxybenzene is a dialkylated derivative of poly(3,4-propylenedioxythiophene) (ProDOT-$R_2$).[32] The band structure of PProDOT-$Hx_2$ is shown in Figure 1, and the high lying HOMO is indicative of the electron-rich nature of polymers incorporating dioxythiophene (XDOT) moieties.

To establish the utility of the CN−PPV motif as the platform for an ideal donor for photovoltaics, here we present a family of soluble, narrow band gap cyanovinylene polymers (shown in Schemes 1 and 2), in which the donor strength and sequence distribution is varied to determine the effect of the donor−acceptor interaction on the electronic properties of the polymers. Such polymers are potentially useful for numerous other applications in addition to photovoltaics, and the electrochromic properties are investigated as proof of the multifunctional nature of this class of polymers.

## Results

**Polymer Synthesis.** The polymers described here were synthesized by three different polymerization routes: Knoevenagel polycondensation, Yamamoto polymerization, and oxidative electropolymerization. Scheme 1 illustrates the synthesis of the polymers realized by Knoevenagel polycondensation. Phenylene diacetonitrile **1** was synthesized by bromomethylation of dialkoxybenzene (all synthetic procedures are in the Supporting Information section) followed by substitution with sodium cyanide or by direct conversion of terephthalaldehyde **2** to the diacetonitrile by reaction with tosyl methyl isocyanide (TosMIC).[33] For alkylthiophene and dioxythiophene monomers, synthesis of diacetonitriles was precluded by their relative instability. Dialdehyde monomers **3** and **4** were readily obtained by lithiation followed by reaction with DMF. For the Knoevenagel polycondensation, the best results were achieved when the reaction was run at reflux in a 1:1 mixture of THF and *tert*-butyl alcohol with at least 1.1 equiv of *t*BuOK per $-CH_2CN$ group, as has been suggested to be the most effective conditions in the literature.[34] It should be noted that this is not a classical A−A + B−B polycondensation as the bis-acetonitrile compound must be deprotonated to be activated for polymerization. The second anion on the compound will not form prior to the first condensation due to the elevated p$K_a$ after deprotonation, which will then cause the polymerization to most likely proceed through coupling of dimer units.

For the preparation of monomers for Yamamoto polymerization or electropolymerization (Scheme 2), the cyanovinylene moiety is set in place by a Knoevenagel reaction prior to polymerization. Synthesis of monoaldehyde precursors **6** and **11** was achieved in an analogous fashion to the dialdehydes **3** and **4** via a lithiation route, whereas monoacetonitrile **5** was synthesized by a Negishi coupling with bromoacetonitrile, similar to that previously described.[16] With the bis-heterocycle-CNV monomers (**7**, **9**, **12**), electropolymerization could directly be achieved (described in the Supporting Information). Prior to Yamamoto coupling polymerization, the bromination of **7** to yield monomer **8** was carried out in DMF with NBS, as has been shown to be an effective method for the bromination of electron-rich heterocycles.[35] Yamamoto coupling polymerization was selected for **8** on the basis of the extremely mild reaction conditions, which provide compatibility with the nitrile functionality.[36]

**Polymer Characterization.** For the soluble polymers, structures are supported by $^1$H NMR, IR, elemental analysis, and MALDI-MS (full characterization is found in the Supporting Information). All the polymers showed $^1$H NMR spectra that were consistent with data reported in the literature for the parent **CN−PPV** polymer.[37] For the Knoevenagel polymers, analysis by IR spectroscopy showed the disappearance of the saturated nitrile stretch at ∼2250 cm$^{-1}$ in the monomer and the appearance of a peak at ∼2210 cm$^{-1}$, characteristic of a cyanovinylene moiety. Analysis by MALDI-MS served to support the proposed structures and Figure 2 shows the spectra for **PProDOT-$Hx_2$:CN−PPV** and **PBProDOT-$Hx_2$:CNV** as representative examples. Figure 2a shows the mass spectrum measured for **PProDOT-$Hx_2$:CN−PPV**, using terthiophene as an electron-transfer MALDI matrix,[38] confirming the presence of polymer chains with masses up to nearly 30,000 amu. The spacing between the major peaks is ∼1738 amu, which corresponds to the calculated molecular weight of two repeat units of the polymer (four condensation reactions), although it is unclear why this is the dominant series in the spectrum. Notice in the inset in Figure 2a that the peaks at *m*/*z* 8693 and 10 432 correspond to $n = 10$ and $n = 12$, respectively, with an additional mass loss of 18, which is observed throughout the dominant series in the spectrum. Small molecules are sometimes

(31) Zerza, G.; Rothler, B.; Sariciftci, N. S.; Gomez, R.; Segura, J. L.; Martin, N. *J. Phys. Chem. B* **2001**, *105*, 4099−4104.
(32) (a) Reeves, B. D.; Grenier, C. R. G.; Argun, A. A.; Cirpan, A.; McCarley, T. D.; Reynolds, J. R. *Macromolecules* **2004**, *37*, 7559−7569. (b) Welsh, D. M.; Kleoppner, L. J.; Madrigal, L.; Pinto, M. R.; Thompson, B. C.; Schanze, K. S.; Abboud, K. A.; Powell, D.; Reynolds, J. R. *Macromolecules* **2002**, *35*, 6517−6525.
(33) van Leusen, A. M.; Oomkes, P. G. *Synth. Comm.* **1980**, *10*, 399−403.
(34) Boucard, V.; Ades, D. Siove, A. Romero, D.; Schaer, M.; Zuppiroli, L. *Macromolecules* **1999**, *32*, 4729−4731.
(35) Mitchell, R. H.; Lai, Y.-H.; Williams, R. V. *J. Org. Chem.* **1979**, *44*, 4733−4735.
(36) (a) Yamamoto, T. *Synlett* **2003** 425−450. (b) Yamamoto, T. *Macromol. Rapid Comm.* **2002**, *23*, 583−606.
(37) Chen, S.-A.; Chang, E.-C. *Macromolecules* **1998**, *31*, 4899−4907.
(38) (a) McCarley, T. D.; Noble, C. O.; DuBois, C. J.; McCarley, R. L. *Macromolecules* **2001**, *34*, 7999−8004. (b) McCarley, T. D.; McCarley, R. L.; Limbach, P. A. *Anal. Chem.* **1998**, *70*, 4376−4379.

*Scheme 2*

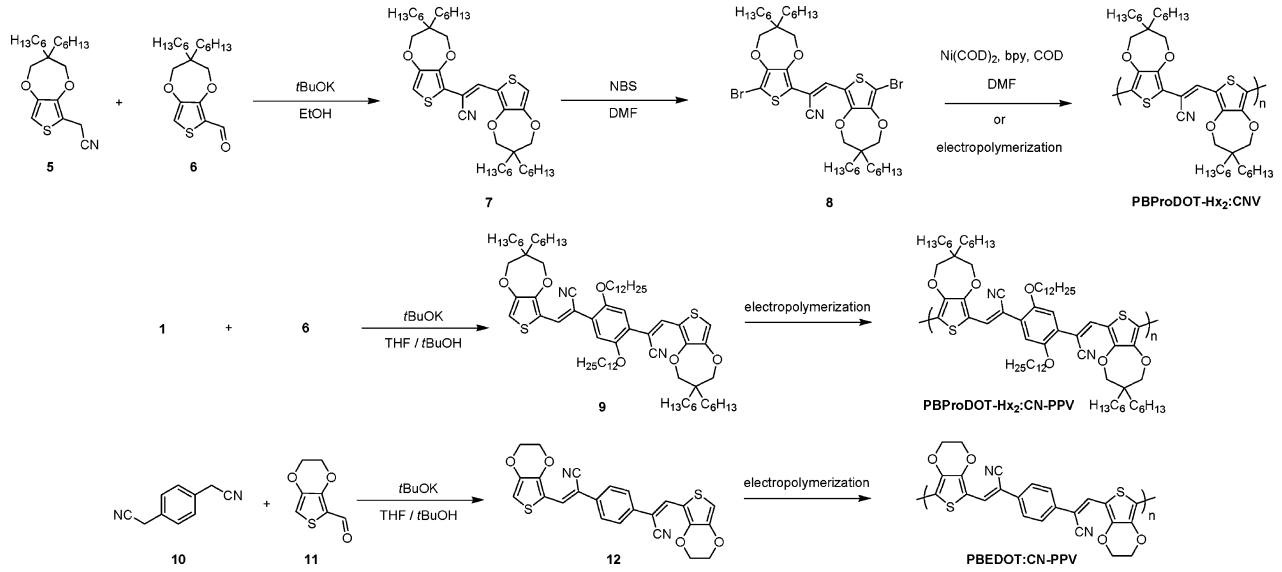


lost under the relatively harsh conditions of MALDI-Qq-TOF, although the precise reason for this mass loss is not clearly understood.

Figure 2b shows the MALDI-MS spectrum for **PBProDOT-Hx$_2$:CNV** in a terthiophene matrix and masses of greater than 10 000 amu are observed. Peak spacing follows a regular pattern with peaks appearing at intervals of 696 amu, which corresponds to the repeat unit molecular weight of the polymer. The inset of Figure 2b also shows that MALDI reveals information about the end groups in the polymer. For $n = 5$, the molecular weights are calculated to be 3482.3, 3561.2, and 3640.1 g/mol for polymer chains with H/H, H/Br, and Br/Br end groups, respectively. In this case, values of 3481, 3560, and 3640 amu are observed, in excellent agreement with the calculated values. Molecular weights were further evaluated by GPC, and Table 1 lists the values estimated by GPC vs polystyrene standards in THF and $CHCl_3$. Importantly, all polymers show number average molecular weights ($M_n$) above 10 000 g/mol relative to polystyrene, and with the exception of **Th−CN−PPV**, the polydispersities are reasonably narrow. For **PBProDOT-Hx$_2$:CNV**, chloroform did not serve as a suitable solvent for GPC.

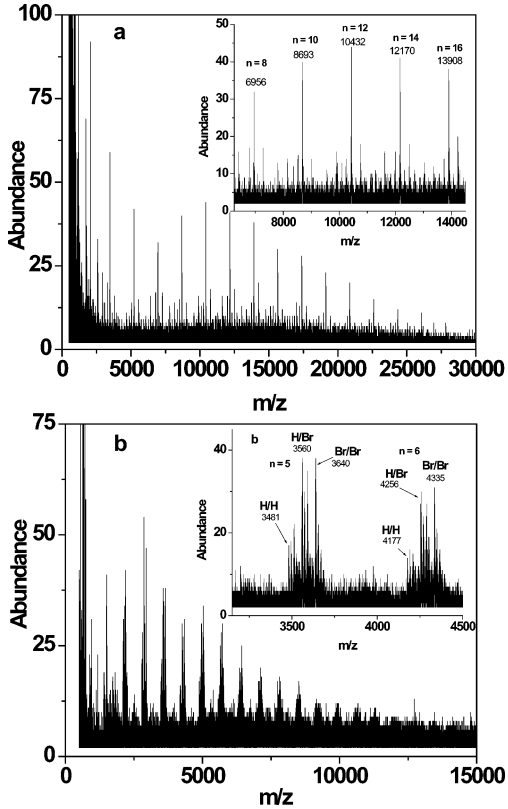


***Figure 2.*** MALDI MS for (a) **PProDOT-Hx$_2$:CN−PPV** and (b) **PBProDOT-Hx$_2$:CNV**. In both cases, terthiophene was used as the matrix.

To investigate the effect of molecular weight on spectral properties, the variation in polymer UV−visible absorbance with elution time was monitored with an inline photodiode array detector during GPC analysis (in $CHCl_3$), for the Knoevenagel polymers (see Supporting Information). This experiment not only allows one to monitor how the polymer electronic properties vary with molecular weight in solution, it gives a direct means to assess the molecular weight at which electronic properties saturate. **PProDOT-Hx$_2$:CN−PPV** shows an absorbance maximum at ∼630 nm for fractions with molecular weights >16 000 g/mol, whereas at a molecular weight of 6000 g/mol, a blue-shifted $\lambda_{max}$ is found at 573 nm, which indicates that the electronic properties of the polymer are no longer saturated for this polymer which has ∼14 aromatic rings. At this low degree of polymerization, the absorption profile of the polymer also changes, showing a single peak, rather than the two peaks observed for the higher molecular weight fractions (see also Figure 3b). For **Th−CN−PPV** the spectrum extracted at the elution peak (14 900 g/mol) shows a maximum at 504 nm, and higher molecular weight fractions show maxima at 513 and 509 nm, whereas the fraction with a molecular weight of 6400 shows a maximum at 496 nm. The relative independence of absorption maximum and curve shape on molecular weight suggest that the optical properties appear to be saturated even at low molecular weights for **Th−CN−PPV**. Similar behavior is observed for **CN−PPV**, as the absorption spectra do not show any significant deviation in absorbance maximum or curve shape for molecular weights between 41 000 and 6200 g/mol.

**Polymer Optical Properties.** Figure 3 shows a comparison of the solution absorption spectra of the soluble ProDOT

***Table 1.*** GPC Estimated Polymer Molecular Weights in THF and $CHCl_3$[a]

| polymer (GPC solvent) | $M_n$ (g/mol) | $M_w$ (g/mol) | PDI | $\lambda_{abs}$ (nm) | $\lambda_F$ (nm) ($\phi_F$) |
|---|---|---|---|---|---|
| **PProDOT-Hx$_2$:CN−PPV** (THF) | 17 400 | 26 300 | 1.51 | 627 | 660 (0.11)[b] |
| **PProDOT-Hx$_2$:CN−PPV** ($CHCl_3$) | 14 700 | 28 700 | 1.95 | | |
| **Th−CN−PPV** (THF) | 25 500 | 102 500 | 4.02 | 522 | 680 (0.036)[c] |
| **Th−CN−PPV** ($CHCl_3$) | 12 500 | 53 000 | 4.25 | | |
| **CN−PPV** (THF) | 13 700 | 29 900 | 2.17 | 463 | 557 (0.050)[c] |
| **CN−PPV** ($CHCl_3$) | 10 900 | 24 400 | 2.24 | | |
| **PBProDOT-Hx$_2$:CNV** (THF) | 14 300 | 40 000 | 2.80 | 610 | 723 (0.033)[b] |

[a] Also shown are polymer absorption and emission data collected in toluene solution. [b] Zinc phthalocyanine in pyridine, $\lambda_{ex} = 610$ nm, $\phi_F = 0.30$. [c] Zinc tetraphenylporphyrin in toluene, $\lambda_{ex} = 420$ nm, $\phi_F = 0.033$.

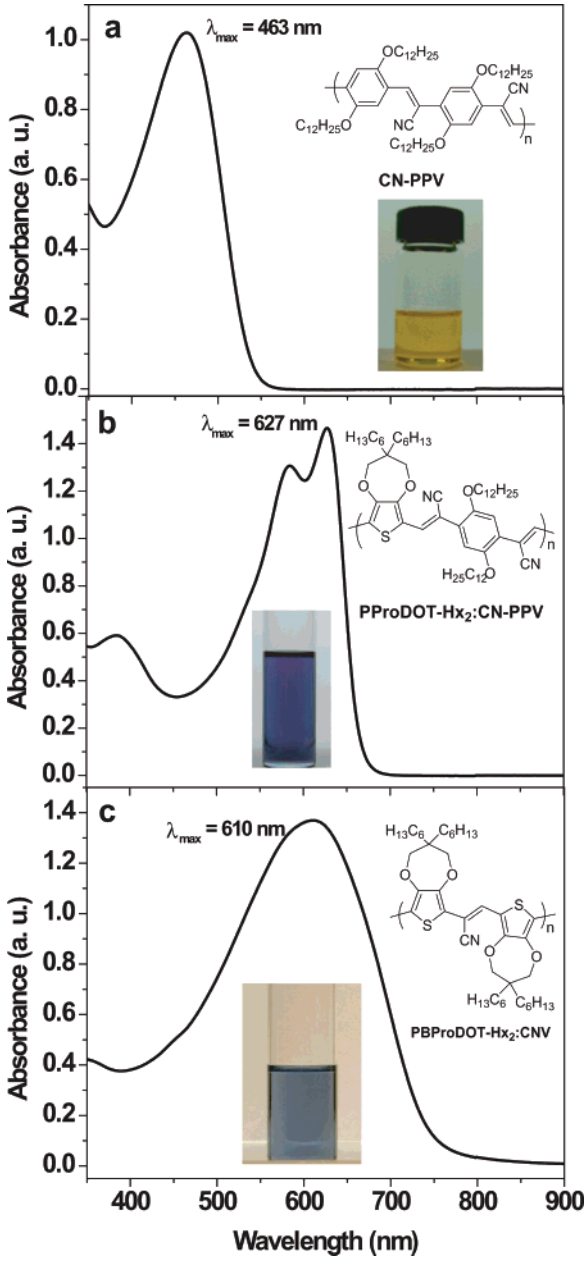


***Figure 3.*** Solution absorbance of CN−PPV analogues in toluene. (a) **CN−PPV**, (b) **PProDOT-Hx$_2$:CN−PPV**, (c) **PBProDOT-Hx$_2$:CNV**.

containing polymers relative to **CN−PPV** in toluene along with a photograph of each solution. It can be seen that with the polymers based on the strongest donor−acceptor interaction, a deep blue is achieved due to the red-shifted absorbance, which is in stark contrast to the orange-yellow **CN−PPV** solution. Table 1 lists the maxima for absorption and emission of all the soluble polymers in toluene solution along with the emission quantum yield.

To optically evaluate the magnitude of the band gap, the thin film absorbance is measured as shown in Figure 4 for either spin cast films or electrodeposited and charge neutralized films. Observe that the optical band gaps range from 2.1 to 1.5 eV, with the parent **CN−PPV** possessing the largest band gap. Replacing one dialkoxybenzene in **CN−PPV** with an alkyl thiophene in the case of **Th−CN−PPV** results in a decrease in the optical band gap from 2.1 to 1.8 eV as has been observed previously for a closely related polymer structure[18] due to the increased donor−acceptor interaction with the more electron-rich alkylthiophene. The propylenedioxythiophene iterations of **CN−PPV** result in similar decreases in the optical band gap as observed for the cases of **PProDOT-Hx$_2$:CN−PPV**, **PBProDOT-Hx$_2$:CN−PPV**, and **PBProDOT-Hx$_2$:CNV** with band gaps of 1.7, 1.6, and 1.5 eV, respectively. Moving to the even more electron-rich EDOT based polymer **PBEDOT:CN−PPV** does not further decrease the optical band gap beyond the observed value of 1.5 eV. Notice that in the case of the electrodeposited films (Figure 4d−f) that the residual absorbance at long wavelengths is attributed to scattering induced by the rough ITO substrate. The thin film absorption coefficients at $\lambda_{max}$ of the polymers were estimated to be on the order of $2 \times 10^4$ $cm^{-1}$ in all cases, calculated using thicknesses measured by profilometry. This absorption coefficient indicates that the polymers are absorbing strongly at low energies and compares favorably with the high absorption coefficients reported for many conjugated polymers.[2h]

**Polymer Electrochemistry.** As a more complete means of mapping the band structures of the polymers and gaining a deeper understanding of the electrochromic and photovoltaic properties, electrochemical measurements were employed to estimate the magnitude of the band gap and the absolute energies of the HOMO and LUMO levels. Here, cyclic voltammetry (CV) and differential pulse voltammetry (DPV) were employed for the analysis of the polymer thin films which were either electrodeposited or solution cast on Pt. Results for all polymers are presented in the Supporting Information, and all electrochemical results are summarized in Table 2. In most cases, the electrochemically determined band gaps were found to be larger than the optically determined band gaps and the band gaps determined by CV were found to be larger than those estimated from DPV. The lack of precise agreement between band gap values determined by these three methods has been observed previously with CNV polymers.[16]

Close examination of the results presented in Table 2 and summarized pictorially in Figure 5 demonstrates the structure−property relationships evident in this polymer family. First, as

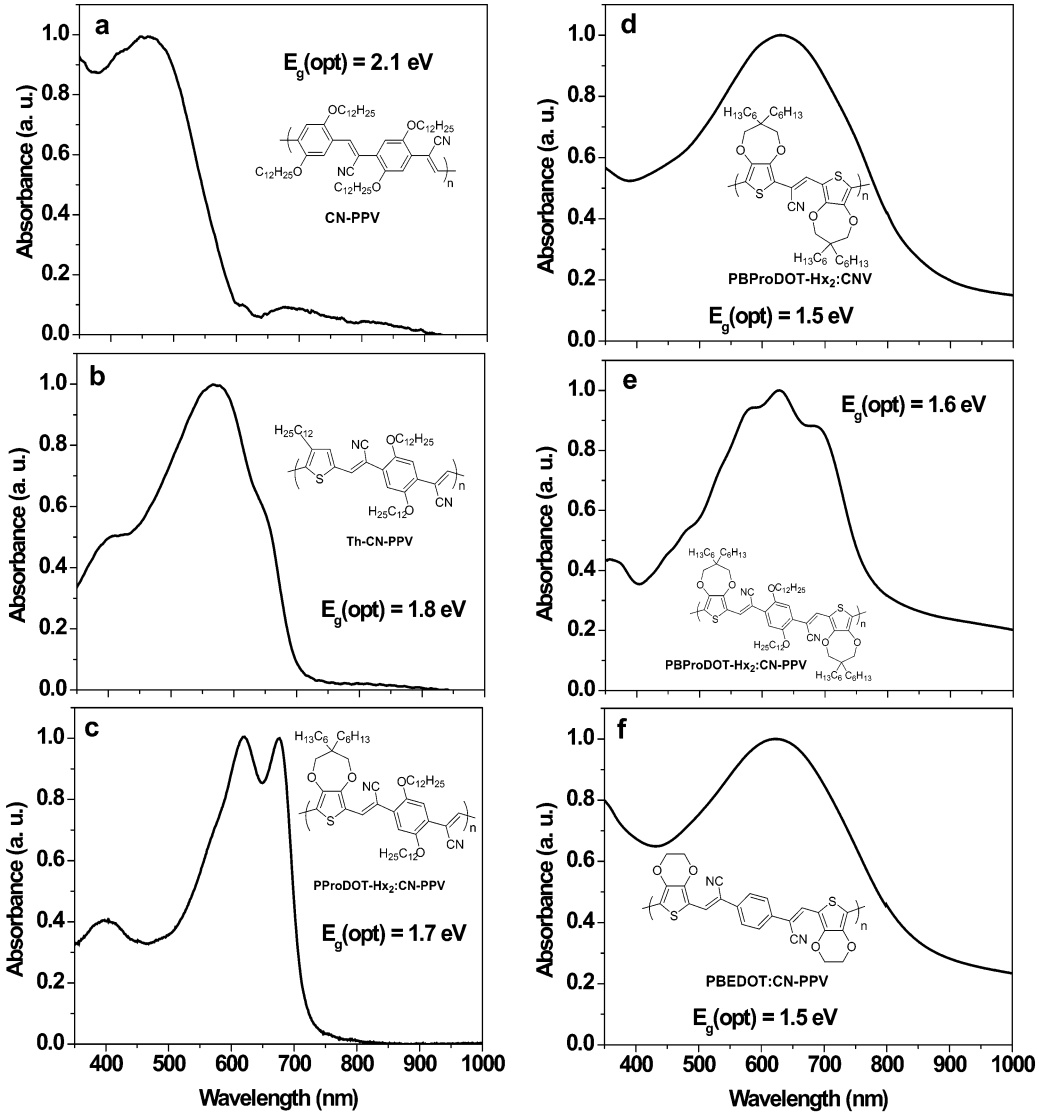


***Figure 4.*** Normalized thin-film optical absorbance of CN−PPV analogues with their respective band gaps as estimated from the onset of the $\pi-\pi^*$ transition. (a) Solution cast **CN−PPV**, (b) solution cast **Th−CN−PPV**, (c) solution cast **PProDOT-Hx$_2$:CN−PPV**, (d) electrodeposited **PBProDOT-Hx$_2$:CNV**, (e) electrodeposited **PBProDOT-Hx$_2$:CN−PPV**, and (f) electrodeposited **PBEDOT:CN−PPV**.

***Table 2.*** Comparison of Electrochemically and Optically Determined Polymer Band Structures[a]

| polymer | $E_{ox}$ onset (CV) V | HOMO (CV) eV | $E_{red}$ onset (CV) V | LUMO (CV) eV | $E_g$ (CV) eV | $E_{ox}$ onset (DPV) V | HOMO (DPV) eV | $E_{red}$ onset (DPV) V | LUMO (DPV) eV | $E_g$ (DPV) eV | $E_g$ (optical) eV |
|---|---|---|---|---|---|---|---|---|---|---|---|
| **CN−PPV** | 1.0 | 6.1 | −1.7 | 3.4 | 2.7 | 1.0 | 6.1 | −1.7 | 3.4 | 2.7 | 2.1 |
| **Th−CN−PPV** | 0.9 | 6.0 | −1.6 | 3.5 | 2.5 | 0.9 | 6.0 | −1.5 | 3.6 | 2.4 | 1.8 |
| **PProDOT-Hx$_2$:CN−PPV** | 0.7 | 5.8 | −1.6 | 3.5 | 2.3 | 0.6 | 5.7 | − | − | − | 1.7 |
| **PBProDOT-Hx$_2$:CNV (echem)** | 0.3 | 5.4 | −1.5 | 3.6 | 1.8 | 0.2 | 5.3 | −1.6 | 3.5 | 1.8 | 1.5 |
| **PBProDOT-Hx$_2$:CNV (drop cast)** | 0.3 | 5.4 | −1.5 | 3.6 | 1.8 | 0.3 | 5.4 | −1.5 | 3.6 | 1.8 | 1.5 |
| **PBProDOT-Hx$_2$:CN−PPV** | 0.3 | 5.4 | −1.7 | 3.4 | 2.0 | 0.3 | 5.4 | −1.6 | 3.5 | 1.9 | 1.6 |
| **PBEDOT:CN−PPV** | −0.3 | 4.8 | −1.5 | 3.6 | 1.2 | −0.4 | 4.7 | −1.4 | 3.7 | 1.0 | 1.5 |

[a] All potentials are reported vs. Fc/Fc$^+$ and all HOMO and LUMO energies are derived from the electrochemical data based on the assumption that the Fc/Fc$^+$ redox couple is 5.1 eV relative to vacuum.

all of the polymers are donor−acceptor polymers in which the acceptor is CNV, the LUMO energy is relatively constant across the series, as expected. The measured LUMO energies for all the polymers fall between 3.4 and 3.7 eV, considering both CV and DPV measurements. As the proportion of electron-rich heterocycle incorporated into the polymer is increased, the HOMO is observed to undergo a concomitant increase in energy level. Looking at the HOMO energies, the value stays essentially constant for **Th−CN−PPV** relative to **CN−PPV** at ∼6 eV, despite the addition of the more electron-rich 3-alkylthiophene. Comparing **PProDOT-Hx$_2$:CN−PPV** with its direct analogue **Th−CN−PPV**, the HOMO energy increases from 6 to 5.7 eV upon replacing alkylthiophene with the more electron-rich ProDOT-Hx$_2$. There is even a more marked change when progressing from **PProDOT-Hx$_2$:CN−PPV** to **PBProDOT-Hx$_2$:CN−PPV** in which the HOMO energy increases from 5.7

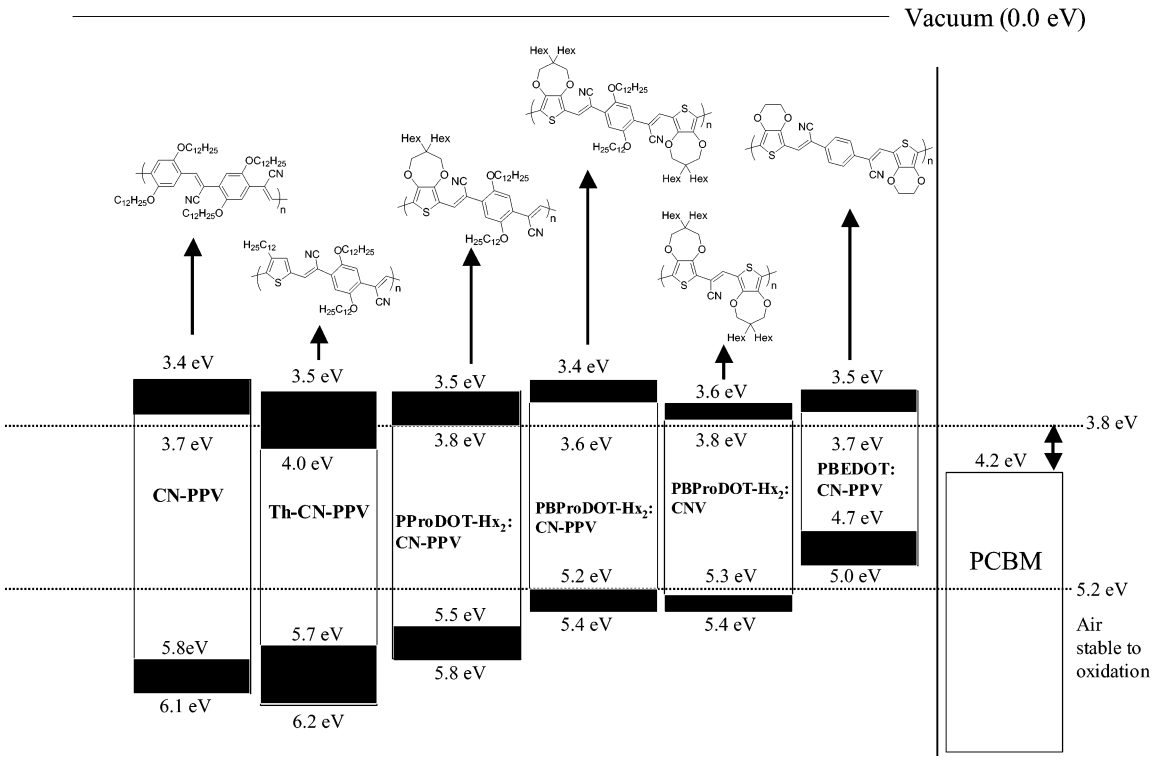


***Figure 5.*** Summary of polymer band structures incorporating optical and electrochemical data. Shaded areas represent the differences between optically and electrochemically determined band gaps, with the optical band gap centered around the baricenter of the overall band gap.

to 5.4 eV based on the equivalent of substituting a BiProDOT-$Hx_2$ moiety into the repeat unit. The HOMO energy of **PBProDOT-$Hx_2$:CNV** remains at essentially the same level as **PBProDOT-$Hx_2$:CN−PPV**, as the HOMO appears to be determined by the electron-rich ProDOT in either case, suggesting that a limiting value for the band gap of polymers based on ProDOT as the donor and CNV as the acceptor is reached at 1.5−1.6 eV. A similar band gap limiting phenomena was previously observed for polymers based on EDOT and CNV in which the inherent HOMO energy of EDOT and LUMO energy of CNV could lead to a donor−acceptor interaction strong enough to reduce the band gap to a value no lower than 1.1 eV.[16] Interestingly, **PBEDOT:CN−PPV** is the only polymer of this family to have a HOMO energy above 5.2 eV, at ∼4.9 eV. This is further evidence that EDOT is a stronger donor than ProDOT. As discussed earlier, **PBProDOT-$Hx_2$:CN−PPV** and **PBEDOT:CN−PPV** have similar optical band gaps (1.6 and 1.5 eV repectively), however the effect of the powerful donor nature of EDOT is clearly observable when examining the HOMO energy measured electrochemically. It is evident that **PBEDOT:CN−PPV** is 0.6−0.7 V easier to oxidize than **PBProDOT-$Hx_2$:CN−PPV**. As such, one can conclude that ProDOT is more effective than EDOT for the synthesis of soluble narrow band gap polymers that are air stable. The accessibility of symmetrically substituted and easy to handle ProDOT derivatives with solubilizing alkyl chains is another advantage of ProDOT over EDOT. Overall, **PBProDOT-$Hx_2$:CN−PPV** and **PBProDOT-$Hx_2$:CNV** come the closest to approaching the ideal electron donor (Figure 1) for PCBM. Especially for the case of **PBProDOT-$Hx_2$-CNV**, the band edges almost perfectly overlap the defined energies for the HOMO and LUMO of the ideal polymer.

**Polymer Spectroelectrochemistry and Colorimetry.** From an application standpoint, spectroelectrochemical measurements offer a direct means of evaluating the electrochromic properties of a conjugated polymer. On a deeper level, such measurements ascertain the relative donor or acceptor character of a polymer based on the charge-carrier induced spectral changes that occur upon oxidation and/or reduction. Figure 6 shows the oxidative spectroelectrochemistry for **PProDOT-$Hx_2$:CN−PPV** and **PBProDOT-$Hx_2$:CNV** films. In Figure 6a, it can be seen that in the neutral form of **PProDOT-$Hx_2$:CN−PPV** (+0.15 V vs. $Fc/Fc^+$), a strong absorption is observed, centered at 600 nm, that corresponds to the $\pi-\pi^*$ transition of the polymer and imparts a deep blue color to the film. Upon increasing the potential in a stepwise fashion (50 mV steps), the $\pi-\pi^*$ transition is observed to bleach with concomitant formation of lower energy charge-carrier associated peaks in the near-infrared. The neutral polymer's optical spectrum is invariant from +0.15 to +0.45 V, followed by a decrease in the $\pi-\pi^*$ transition at +0.5 V (as indicated in Figure 6a), and the film is fully oxidized by +0.85 V.

During this process, the polymer is undergoing p-type doping, in which the polymer is converted to a more conductive, doped form. Throughout this process, the polymer thin film is observed to become gradually more transparent and, at +0.85 V the polymer is a transmissive sky blue. The color change observed here is similar to that observed in PEDOT, but the applied potentials required to affect bleaching are considerably higher, as the spectrum of PEDOT is observed to evolve at potentials as low as −0.4 V vs. $Fc/Fc^+$.[39] From an electrochromic point of view, **PProDOT-$Hx_2$:CN−PPV** is an organic soluble form of PEDOT that has an air stable neutral form. The relatively weak near-infrared absorbance in the oxidized polymer is perhaps evidence that relatively few charge carriers are induced in the polymer backbone upon p-doping.

(39) Kumar, A.; Welsh, D. M.; Morvant, M. C.; Piroux, F.; Abboud, K. A.; Reynolds, J. R. *Chem. Mater.* **1998**, *10*, 896−902.

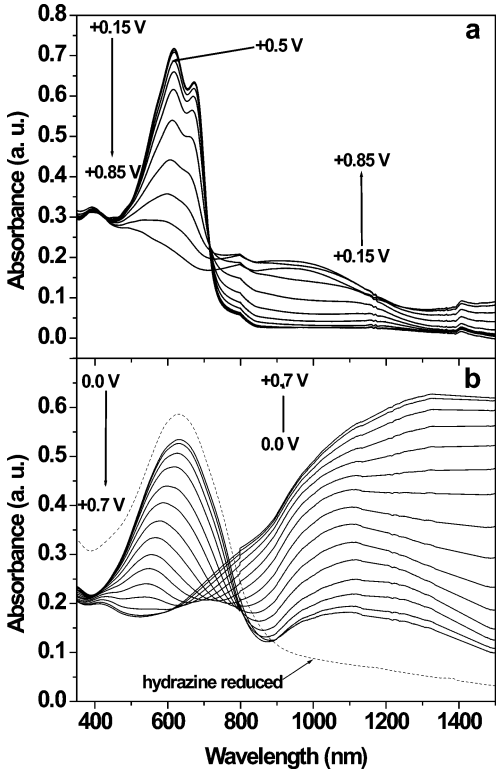


***Figure 6.*** Spectroelectrochemistry of (a) **PProDOT-Hx$_2$:CN−PPV** and (b) **PBProDOT-Hx$_2$:CNV**. Polymer films were cast from dichloromethane solution (1% w/w) onto ITO coated glass. All potentials are reported vs $Fc/Fc^+$. The supporting electrolyte consisted of 0.1 M TBAP/acetonitrile. In both cases, the potential was increased in 50 mV steps. Note that the fully neutral spectrum for **PBProDOT-Hx$_2$-CNV** is only attainable by reducing the film with hydrazine, indicating that once the film has been cycled, it is difficult to fully neutralize the polymer electrochemically.

Figure 6b shows the spectroelectrochemical series for **PBProDOT-Hx$_2$:CNV**. Here, the neutral polymer is also deep blue and upon oxidation the visible absorption is gradually bleached, resulting in a polymer that is transmissive sky blue in the oxidized form. The two main differences observed for **PBProDOT-Hx$_2$:CNV** relative to **PProDOT-Hx$_2$:CN−PPV** are a lower switching potential at 0.0 V (as opposed to 0.5 V) and a much more intense near-infrared absorption induced upon doping. The lower switching potential is expected based on the results presented in Table 2, which indicate a higher lying HOMO for **PBProDOT-Hx$_2$:CNV**. The much more intense absorption band in the near-infrared suggests that a higher doping level is achieved in **PBProDOT-Hx$_2$:CNV** relative to **PProDOT-Hx$_2$:CN−PPV**. This phenomenon could be due to some inherent property of the two films or it could simply be attributed to the fact that **PBProDOT-Hx$_2$:CNV** is stable over a wider range of potentials anodic of the onset of oxidation, possibly allowing higher doping levels.

The spectral changes observed upon reduction were also measured for the family of polymers under an oxygen and water free environment in an argon-filled glovebox. Figure 7 shows the reductive spectroelectrochemical series for **PProDOT-Hx$_2$:CN−PPV** (spectra for **Th−CN−PPV**, **CN−PPV**, and **PBEDOT:CN−PPV** are shown in the Supporting Information), which showed the most pronounced spectral changes upon reduction. In all cases, at increasingly cathodic potentials, the neutral $\pi-\pi^*$ transition is observed to bleach at the expense of lower energy charge-carrier associated transitions. These spectral

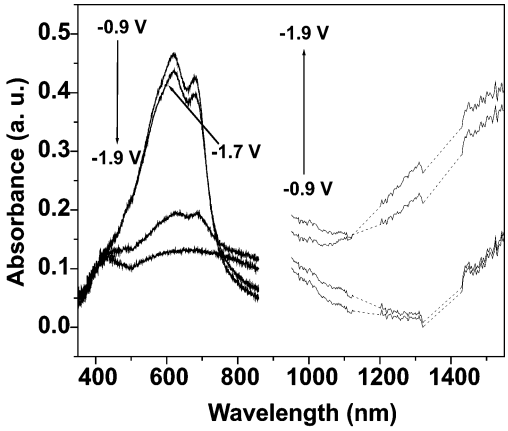


***Figure 7.*** Reductive spectroelectrochemistry of **PProDOT-Hx$_2$:CN−PPV**. No data is shown between 860 and 950 nm as the detectors do not cover this wavelength range. Potentials were increased in 100 mV steps and all potentials are reported vs $Fc/Fc^+$. The supporting electrolyte consisted of 0.1 M $TBAPF_6$/acetonitrile. Note that the data between 1125 and 1200 nm as well as 1325−1425 nm (dashed lines) has been removed due to overtones that appear to be attributed to acetonitrile, which appear when using a fiber optic spectrometer.

changes are reflected in reversible color changes in the films, and thus considering both the oxidative and reductive spectroelectrochemical results, a continuum of color states is observed for each polymer throughout the electroactive range. The range of colors attainable from each polymer has been quantified by colorimetric analysis,[40] and the specific color states for the oxidized, neutral, and reduced forms of each polymer are listed in the form of L*a*b* coordinates in the Supporting Information. In general, the polymer films are highly colored in the absorptive neutral form, ranging from blue to orange. Upon oxidation and reduction, the films become more transmissive across the visible region and are typically a color-neutral gray. For the electropolymerized polymer **PBProDOT-Hx$_2$:CN−PPV**, films thick enough for spectroelectrochemistry and colorimetry were not formed, precluding the collection of data.

The question of interest is whether the above spectral changes upon reduction can be attributed to a true n-type doping or not. Previous work in our group has indicated that simple electrochemical reduction in conjugated polymers cannot be directly attributed to an n-type doping processes.[16,41] For a polymer to be considered n-doped, not only must the polymer show a reduction, but the polymer must show evidence for charge carrier formation on reduction, as can be assessed by spectroelectrochemistry or in-situ conductivity measurements. The strong increase in the near-infrared absorption of the polymers upon reduction suggests that a true n-type doping process is occurring. Previous work in our group[16] on electropolymerizable cyanovinylene polymers has relied on in situ conductivity measurements to establish n-doping and these measurements showed that the conductivity in the polymers is best attributed to a redox or hopping type conductivity upon reduction as the carrier mobility is likely rather low. From the practical standpoint of application of the polymers as electron donors in solar cells, the main interest in the spectroelectrochemical results presented here is

(40) Thompson, B. C.; Schottland, P.; Zong, K.; Reynolds, J. R. *Chem. Mater.* **2000**, *12*, 1563−1571.
(41) (a) DuBois, C. J.; Reynolds, J. R. *Adv. Mater.* **2002**, *14*, 1844−1846. (b) DuBois, C. J.; Abboud, K. A.; Reynolds, J. R. *J. Phys. Chem. B* **2004**, *108*, 8550−8557.

that all of the polymers show a strong donor character, as they are readily p-type doped.

**Polymer Photovoltaic Devices.** The polymers described in the previous sections were designed to function as electron donors for a fullerene acceptor in a photovoltaic device. Before incorporating a polymer into a device with PCBM, it is interesting to examine the energetic relationship between the two components in thin films. Proof for charge transfer can be established using a variety of techniques such as light induced electron spin resonance (LESR), photoinduced absorption (PIA), and time-resolved transient absorption (TA).[24] Another simpler technique is photoluminescence (PL) quenching, which was utilized for all the soluble polymers presented here. With the exception of **PBProDOT-Hx$_2$:CNV**, all of the soluble polymers showed photoluminescence in thin films. The PL quenching behavior for **PProDOT-Hx$_2$:CN−PPV** has been previously reported[26] and it was observed that greater than 95% of the PL was quenched in thin film blends with PCBM. Similar results were observed for **Th−CN−PPV** and **CN−PPV** (see Supporting Information).

Bulk heterojunction photovoltaic devices were constructed based on 1:4 (w:w) blends of each soluble polymer with PCBM. In all cases, blends were spin coated from dichlorobenzene and the chosen weight ratio of 1:4 is based on studies in our labs and others that suggests that this weight ratio is the most effective for producing efficient devices with vinylene polymers.[22g,h] The measurement of the incident photon to current efficiency (IPCE) or external quantum efficiency in preliminary devices is crucial, as it can offer strong proof of electron transfer from the polymer to PCBM through a photocurrent action spectrum that strongly parallels the polymer absorption spectrum. It should be noted that these experiments were done under conditions that would allow the fundamental contribution of each polymer to the device to be compared to the others in the family, and as of yet, we have not focused on the practical aspect of optimizing device engineering.

Measurement of IPCE for **Th−CN−PPV**/PCBM (1:4) solar cells (see Supporting Information) in which the active layer was spin coated from dichlorobenzene (30 mg/mL) indicates that the photocurrent matches the polymer absorption spectrum very closely; however, the peak efficiency of only ∼1% indicates that the overall process of photogeneration and collection of charge carriers is not efficient in the devices constructed under the employed conditions. Importantly though, it does appear that the photoexcited polymer is a contributor to the photocurrent in the device. The diode characteristics show an open circuit voltage ($V_{oc}$) of ∼0.45 V with a short circuit current density ($J_{sc}$) of 0.1 mA/cm$^2$ and a fill factor (*FF*) of 0.25 for an overall AM1.5 power conversion efficiency ($\eta_{eff}$) of only 0.01%.

AFM studies of the blends of **Th−CN−PPV** and PCBM spin coated from dichlorobenzene on PEDOT-PSS coated glass revealed that the films had a surface roughness of 3 nm (the film thickness was approximately 50 nm as established by profilometry). However, there appear to be fissures in the surface (see Supporting Information) and it is evident that the film quality in the blends of **Th−CN−PPV** and PCBM is less than optimal. Optimization based on solvent choice, solution concentration, etc., could possibly lead to an improvement in film quality and perhaps device performance.

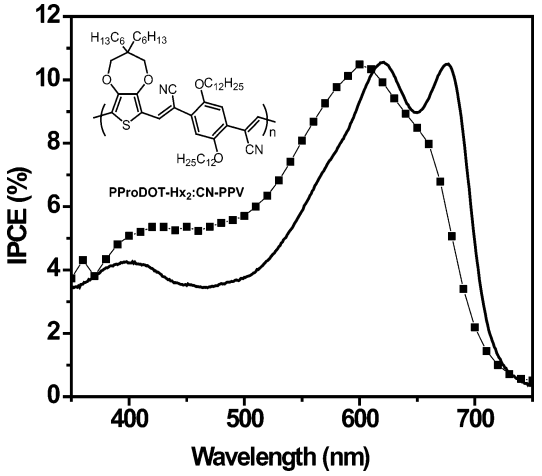


***Figure 8.*** Photocurrent action spectra for a **PProDOT-Hx$_2$:CN−PPV**/PCBM solar cell based on a 1:4 blend (w:w) of polymer and PCBM. Black squares represent the IPCE value at the given wavelength. The solid curve is the absorption spectra of a pristine polymer film shown as reference.

Figure 8 shows the IPCE of a **PProDOT-Hx$_2$:CN−PPV**/PCBM (1:4) solar cell in which the active layer was spin coated from dichlorobenzene (30 mg/mL). The IPCE data indicates that **PProDOT-Hx$_2$:CN−PPV** is acting as a photoexcited electron donor and is thus the major contributor to the photocurrent in the device. The slight blue-shift in the IPCE relative to the polymer absorption spectra is a consequence of blending the polymer with PCBM. The IPCE data shown in Figure 8 is for a representative device, but the observed spectral dependence of the photocurrent is reproducible from device to device. For this same type of device, an AM1.5 efficiency of 0.15% and a $J_{sc}$ of ∼1.3 mA/cm$^2$ were measured, which are reasonable values for an unoptimized device. The low *FF* of only 0.25 is indicative of an unoptimized device with a high series resistance (see Supporting Information for an I−V characteristic).

The surface morphology of **PProDOT-Hx$_2$:CN−PPV**/PCBM (1:4) blends spin coated from 30 mg/mL solutions (dichlorobenzene) was studied on PEDOT-PSS coated glass slides by atomic force microscopy (AFM). The surface roughness is calculated to be only 1 nm, indicating a very smooth surface and on the micron scale the films do not appear to be phase separated. This material shows a superior film quality relative to the devices based on **Th−CN−PPV** and PCBM, which could help to explain the improved performance of **PProDOT-Hx$_2$:CN−PPV** devices relative to **Th−CN−PPV** devices. Films were 50 nm thick as measured by profilometry.

As with **PProDOT-Hx$_2$:CN−PPV**, devices based on **PBProDOT-Hx$_2$:CNV**/PCBM (1:4) gave reasonable photovoltaic performance. A measured *FF* of 0.32 indicates that the devices are operating as somewhat more ideal diodes than seen with the devices based on **PProDOT-Hx$_2$:CN−PPV**. Again, a $J_{sc}$ of ∼1.2 mA/cm$^2$ and a power conversion efficiency of 0.21% are reasonable values for an unoptimized device. The IPCE data for these **PBProDOT-Hx$_2$:CNV** devices were also measured (see Supporting Information) and values of greater than 15% are observed at wavelengths in the UV region of the spectrum. The photocurrent does mirror the polymer absorption near the maximum absorption of the polymer; however, the IPCE at that point is only ∼2%. Such behavior indicates the polymer is not

acting primarily as a photoexcited electron donor for PCBM. Instead, the IPCE data appears to suggest that PCBM is the primary contributor to the photocurrent. A mechanism based on electron transfer from the HOMO of the polymer to the HOMO of photoexcited PCBM may be predominating in this case. Referring to Figure 5, it is clear that the HOMO of **PBProDOT-Hx$_2$:CNV** is higher than the HOMO of **PProDOT-Hx$_2$:CN−PPV**, which may help to drive this inverse mode of solar cell operation in the former case relative to the latter case. By AFM, a very smooth surface is observed for **PBProDOT-Hx$_2$:CNV** blends with PCBM, with a surface roughness calculated to be less than 1 nm. As with the **PProDOT-Hx$_2$:CN−PPV** films discussed above, AFM gives little information about the precise morphology of the **PBProDOT-Hx$_2$:CNV**/PCBM films. However, the relatively smooth and uniform nature of the film surface suggests that there is no macrophase separation in the blend.

For the PVDs based on the soluble narrow band gap polymers presented here, it can be observed that only **PProDOT-Hx$_2$:CN−PPV** and **PBProDOT-Hx$_2$:CNV** gave reasonable photovoltaic performances in devices based on 1:4 blends of polymer and PCBM. In both cases however, efficiencies are hampered by the low Fill Factors, which are indicative of a high resistance in the films and could point toward low hole mobilities as a problematic feature of the devices. Optimization of film composition and morphology and the implementation of so-called post-production treatment strategies[22f] such as thermal and or electrical annealing could serve to optimize the performance of the devices. For **PProDOT-Hx$_2$:CN−PPV** the origin of the photovoltaic activity is clear as evidenced by the IPCE shown in Figure 8, although for **PBProDOT-Hx$_2$-CNV** it is evident that light absorption by PCBM is the primary source for photoinduced charge transfer.

## Summary and Perspective

Here, we have presented a family of soluble dioxythiophene-cyanovinylene polymers and demonstrated the utility of this structural platform for generating materials with tailored electronic properties suitable for a variety of applications such as photovoltaic and electrochromic devices. Cyanovinylene polymers based on ProDOT derivatives are attractive targets because soluble high molecular weight polymers can be realized through either a Knoevenagel or a Yamamoto polymerization to give regiosymmetric polymers with well-defined structures. An advantage of the Knoevenagel route is the robust nature of this high-yielding reaction that gives high molecular weight polymers in the neutral form without the use of metal catalysts that could potentially be trapped in the polymer. On the basis of the polymer band structures shown in Figure 5, a clear correlation can be seen between the donor strength and content in these donor−acceptor polymers and the resulting band structures of the materials. From an electronic point of view, these soluble polymers offer several strengths, which include air-stability (based on a low lying HOMO), a narrow band gap (based on the donor−acceptor interaction), and a sufficiently electron-rich structure to allow them to function as donor materials in solar cells. Relative to the variety of other low band gap polymers reported in the literature this property set appears to make these polymers unique.

From a structural point of view, it is the incorporation of ProDOT as the donor rather than EDOT or thiophene that makes this unique property set possible. As a stronger donor than thiophene (or alkylthiophene), ProDOT imparts a stronger donor−acceptor interaction in combination with acceptors, resulting in polymers with an enhanced electron-rich character and narrower band gaps. At the same time ProDOT monomers substituted with solubilizing groups are symmetrical monomers that overcome the synthetic challenges of 3-alkylthiophenes and do not suffer from the unfavorable steric interactions experienced by 3,4-disubstituted thiophenes. Importantly ProDOT monomers also show several advantages over EDOT as a donor heterocylcle in donor−acceptor polymers. As shown in Figure 5, **PBEDOT:CN−PPV** has a narrower band gap than **PBProDOT-Hx$_2$:CN−PPV** (1.5 eV vs 1.6 eV optically), but the incorporation of the stronger EDOT donor results in a HOMO level of ∼4.9 eV for **PBEDOT:CN−PPV**, which renders the polymer unstable to oxidation under ambient conditions, whereas **PBProDOT-Hx$_2$:CN−PPV** shows a HOMO of 5.4 eV and is stable to oxidation in air. Air stability in the neutral form is a key feature of these materials, which makes them attractive for application in that the polymers can be processed in air prior to device fabrication without fear of oxidation. Ease of symmetrical substitution for solubility in ProDOT is a further advantage relative to EDOT in the context of serving as a building block for soluble polymers.

As a consequence of the described electronic properties, ProDOT-CNV polymers show band gaps of 1.5−1.7 eV, making them near-ideal absorbers of the solar spectrum. Results presented here for unoptimized photovoltaic devices based on **PProDOT-Hx$_2$:CN−PPV** and **PBProDOT-Hx$_2$:CNV** show promise for further development. Although AM1.5 efficiencies of only 0.1−0.2% were observed for these two polymers in 1:4 blends with PCBM, $J_{sc}$ values larger than 1 mA/cm$^2$ suggest that optimization of device engineering could yield effective devices. Further structural optimization of the polymer structures presented here can also seek to overcome such shortcomings as the apparent inability of **PBProDOT-Hx$_2$:CNV** to act as a photoexcited donor for PCBM. Importantly, the efficiencies reported here should not be directly compared to the values approaching 5% that have been obtained for P3HT:PCBM devices,[22i,k] as this well established system has been the focus of intense scrutiny and benefits from years of optimization by numerous research groups. Instead, the photovoltaic properties of the polymers presented here should be compared to the relatively few examples of polymers with band gaps of less than 1.8 eV that have been successfully employed in PCBM-based solar cells. In this case, only one example exists in which device efficiencies have reached 1%, as is the case for a complicated thiophene/pyrrole/benzothiadiazole hybrid polymer (PTPTB, $E_g$ = 1.6 eV), which gave efficiencies of ∼1% under AM1.5 conditions in 1:3 blends (w:w) with PCBM.[30a] However a limitation of PTPTB not suffered by the ProDOT-CNV polymers is the low molecular weight and limited solubility that is found with this polymer.[15]

Beyond the obvious appeal of ProDOT-CNV polymers for photovoltaic devices, the general strengths of these polymers make them appealing as multifunctional materials. Specifically, the electrochromic properties described here illustrate a new class of soluble electrochromic polymer that is colorless/

transmissive in the oxidized state and colored/absorptive in the neutral state. These electrochromic properties make this class of polymer very similar to PEDOT, with the advantage that the polymers have an air-stable neutral state. Interestingly, the CNV polymers presented here also have accessible color states in the reduced form as illustrated by spectroelectrochemistry and colorimetry. These spectroelectrochemical results also indicate the possibility that these polymers can exhibit both p- and n-type doped states, which further increases the range of possible applications with this class of materials. Future synthetic efforts and detailed characterization coupled with device optimization promise to solidify the importance of these ProDOT-CNV polymers as multifunctional conjugated polymers.

**Acknowledgment.** We thank the AFOSR (FA955-06-1-0192) and EIC Laboratories (NASA − NNC05CB23C) for funding this work. B.C.T. thanks the NSF (NSF Graduate Research Fellowship) and Eastman Chemical (Eastman Fellowship in Polymer Science). TDM thanks the NSF for funding (CHE-0074884). Our thanks to Nisha Ananthakrishnan for her assistance with the AFM measurements.

**Supporting Information Available:** Synthetic details and additional polymer characterization not included in the manuscript. This material is available free of charge via the Internet at http://pubs.acs.org.

JA061274A